

XAFS Study on Chlorination of Y_2O_3 in LiCl-KCl-ZrCl₄ Melt

Yoshihiro Okamoto^a, Tsuyoshi Yaita^a, Hideaki Shiwaku^a, and Shinichi Suzuki^b

^a Quantum Beam Science Directorate, Japan Atomic Energy Agency, Kouto 1-1-1, Sayo-cho, Hyogo 679-5148, Japan

^b Nuclear Science and Engineering Directorate, Japan Atomic Energy Agency, Shirakata-Shirane 2-4, Tokai-mura, Ibaraki 319-1195, Japan

Reprint requests to Y. O.; E-mail: okamoto@molten.tokai.jaeri.go.jp

Z. Naturforsch. **63a**, 735 – 738 (2008); received April 24, 2008

The chlorination reaction of Y_2O_3 with $ZrCl_4$ in LiCl-KCl eutectic melt was investigated by X-ray absorption fine structure (XAFS) technique. The chlorination reaction was observed between 773 K and 823 K as the 1st peak shift of the Fourier transform magnitude function $|FT(k^3\chi(k))|$. The peak corresponding to the nearest $Y^{3+}-Cl^-$ correlation was observed in the XAFS analysis at 823 K as the result of the chlorination. It was confirmed that the mixture melts after the reaction is almost equivalent to a molten 5% YCl_3 -(LiCl-KCl eutectic) mixture.

Key words: XAFS; Molten Salt; Chlorination; Nuclear Fuel Cycle.

1. Introduction

Molten salt is an attractive medium for many industrial processes. Also in the nuclear fuel cycle, it has been used as a solvent of the pyrochemical reprocessing of spent nuclear fuels [1]. For example, LiCl-KCl eutectic mixture is the most promising candidate of a solvent. Many kinds of reactions in this solvent are performed in pyrochemical processes. Chlorination of the oxide fuel must be an important reaction in pyrochemistry, since molten chloride mixtures are widely used in reprocessing.

Sakamura et al. [2] proposed the chlorination method using $ZrCl_4$ in the chloride melt. Some oxides were successfully chlorinated with $ZrCl_4$ in an LiCl-KCl eutectic melt. In the present work, we studied the chlorination of Y_2O_3 in a molten LiCl-KCl- $ZrCl_4$ mixture by X-ray absorption fine structure (XAFS) technique.

2. Experimental

Y_2O_3 was selected as a starting oxide and YCl_3 was expected as a product. We can obtain both Y and Zr XAFS patterns in single scan, since the Y K-edge energy (17.080 keV) is close to the Zr K-edge energy (17.998 keV). This means that oxidization of $ZrCl_4$ is also detected in addition to the chlorination of Y_2O_3 . LiCl-KCl eutectic melt was selected as the solvent.

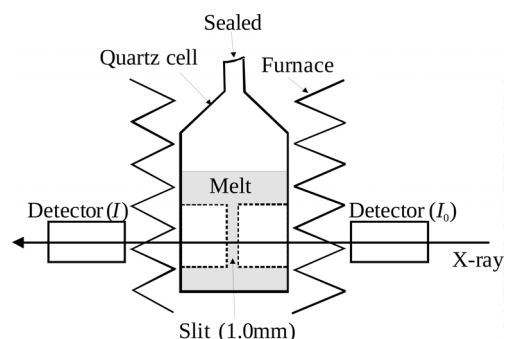
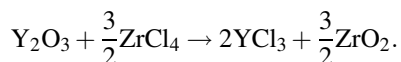


Fig. 1. Scheme of the high-temperature molten salt XAFS measurement.

We already reported [3] the XAFS result of molten YCl_3 and its mixture melts with LiCl-KCl eutectic. An XAFS function similar to that of the YCl_3 -(LiCl-KCl eutectic) mixture is expected as the result of the chlorination reaction for Y_2O_3 .

The high-temperature molten salt XAFS system used is described in [4]. An outline of the XAFS measurement system is shown in Figure 1. The electric furnace is located between two detectors to obtain X-ray intensity before and after the sample (I_0 and I). The XAFS spectrum (absorbance, μt) is obtained from $-\ln(I/I_0)$. The sample is sealed in the quartz cell under reduced pressure. The cell is a quartz tube having a narrow slit (1.0 mm width) designed for molten salt XAFS measurements [5]. The expected reaction in the

molten LiCl-KCl eutectic melt is as follows:



Thus, starting materials were Y_2O_3 , ZrCl_4 and LiCl-KCl eutectic. At first, 10% ZrCl_4 -(LiCl-KCl eutectic) was prepared by melting ZrCl_4 in LiCl-KCl eutectic melt, since ZrCl_4 reacts easily with oxygen. Secondly, dried Y_2O_3 powder was mixed with the ZrCl_4 -LiCl-KCl mixture. A molar ratio $\text{ZrCl}_4/\text{Y}_2\text{O}_3 = 2$, larger than the ideal ratio 1.5, was used, because a loss of ZrCl_4 was expected.

The XAFS measurements using a transmission technique were performed at the BL27B beamline of the Photon Factory in the Institute of Materials Structure Science of the High Energy Accelerator Research Organization (KEK) in Tsukuba, Japan. The radiation was monochromatized using an Si(111) double monochromator. A fixed scan time with 1.0 s per data point ranging from 16.89 keV to 18.92 keV was used to obtain the XAFS spectra. The computer program WinXAS ver. 3.1 [6] was used to analyze the XAFS data. Processing of the high-temperature XAFS data is summarized in [3].

3. Results and Discussion

Figure 2 shows the thermal history of the sample during the XAFS measurement. At first, the XAFS pattern at room temperature was obtained before heating (XAFS-B). After heating up to 773 K, three XAFS measurements were performed at the constant temperature for the liquid phase. The 1st XAFS measurement for the liquid phase, XAFS-M1, was at 773 K during the heating process. Then the sample was heated up to and kept at 823 K. The XAFS-M2 measurement was

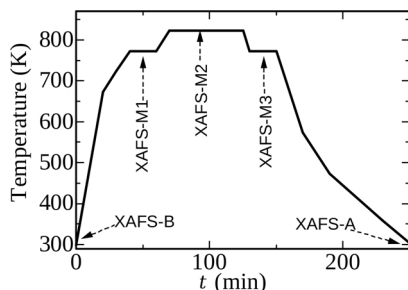


Fig. 2. Thermal history of the sample. The XAFS measurements were performed before heating (XAFS-B), at 773 K (XAFS-M1 and XAFS-M3), at 823 K (XAFS-M2) and after cooling (XAFS-A), respectively.

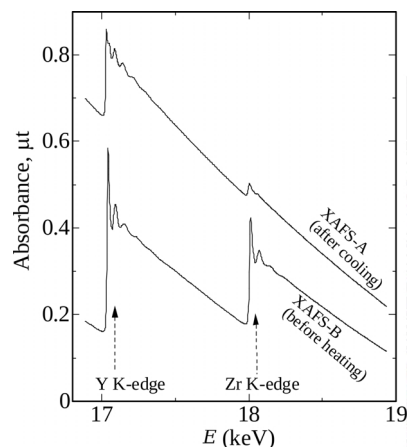


Fig. 3. Raw XAFS spectra of the Y K-edge and Zr K-edge before heating and after cooling.

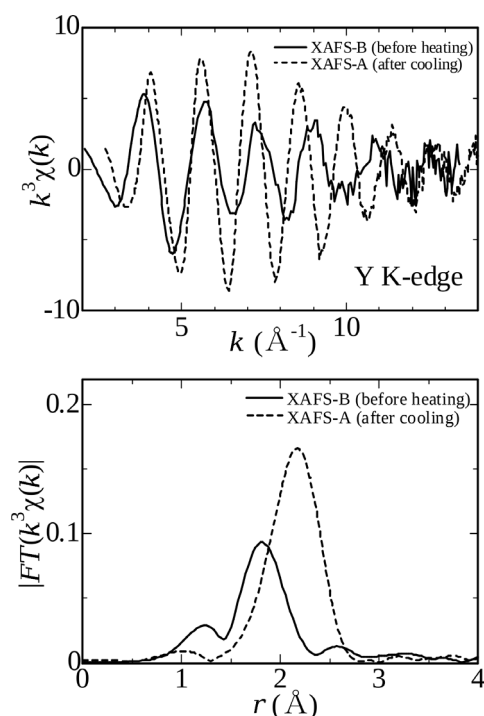


Fig. 4. XAFS function $k^3\chi(k)$ and Fourier transform magnitude function $|FT(k^3\chi(k))|$ of the Y K-edge before heating and after cooling.

performed at 823 K. Thereafter, the sample was cooled down to 773 K and kept there to perform the XAFS-M3 measurement. Finally, the XAFS pattern at room temperature was obtained after cooling (XAFS-A).

Two solid state XAFS spectra, XAFS-B and XAFS-A, are shown in Figure 3. The Zr K-edge

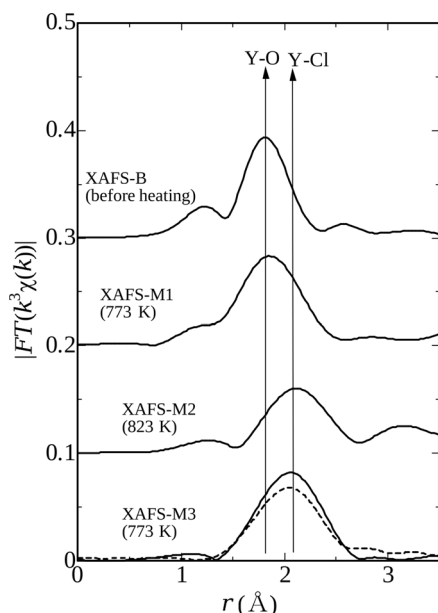


Fig. 5. Fourier transform magnitude function $|FT(k^3\chi(k))|$ of the Y K-edge before heating and after cooling. The dashed line shows the XAFS result of molten 5% YCl_3 in the LiCl-KCl eutectic [3].

jump became very small after cooling (XAFS-A). This means that material containing Zr disappeared from the bulk of the sample. On the other hand, the Y K-edge jump of XAFS-A shows that a reasonable amount of Y exists in the bulk of the mixture melt after the reaction. Figure 4 shows the Y K-edge XAFS function $k^3\chi(k)$ and the Fourier transform magnitude $|FT(k^3\chi(k))|$ of the XAFS-B and the XAFS-A results. It is clear that the local structure around the Y atom changes by heating. The XAFS function and its Fourier transform magnitude of the XAFS-A are completely different from those of XAFS-B. The 1st peak of the magnitude $|FT(k^3\chi(k))|$ of XAFS-A is clearly longer than that of XAFS-B.

The Fourier transform magnitudes $|FT(k^3\chi(k))|$ at liquid state are shown in Fig. 5, together with those of XAFS-B (the starting solid sample). The XAFS-M1 result at 773 K in the heating process shows that the 1st peak corresponds to the nearest Y-O correlation. The peak position of XAFS-M1 is almost the same as that of XAFS-B. This means that the nearest neighbour atom around the Y absorber is still oxygen in the XAFS-M1 result. A clear change of the 1st peak position was observed in the XAFS-M2 result at 823 K. Here the 1st peak position was by ca. 0.3 Å longer than that of the XAFS-M1 result. The value of 0.3 Å shows

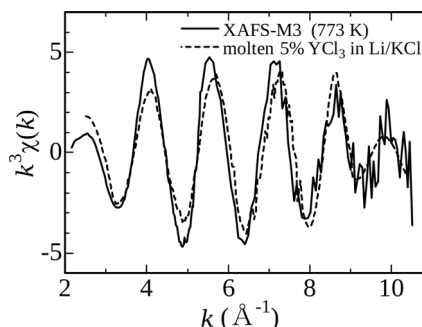


Fig. 6. XAFS function $k^3\chi(k)$ of the Y K-edge for the XAFS-M3 result, together with the XAFS result of molten 5% YCl_3 in the LiCl-KCl eutectic [3].

that the chlorination reaction occurred in the melt. According to the curve fitting analysis of the XAFS-M1 data, the nearest Y-O distance was 2.36 Å, which is very close to the sum of the covalent radii (2.35 Å) of Y and O. On the other hand, the nearest Y^{3+} -Cl⁻ distance from the XAFS-M2 data was 2.67 Å, which is almost the same as the sum of the ionic radii (2.71 Å) of Y^{3+} and Cl⁻. In addition, this value is close to the XAFS result (2.68–2.72 Å) of molten YCl_3 systems [3] and the result (2.71 Å) of neutron diffraction studies [7]. The XAFS-M3 result at 773 K in the cooling process shows the 1st peak at almost the same position as the XAFS-M2 result. The XAFS-M3 result is different from the XAFS-M1 result in spite of the same temperature. This suggests that the chlorination reaction is irreversible.

The $|FT(k^3\chi(k))|$ function of the Y K-edge XAFS for molten 5% YCl_3 in LiCl-KCl eutectic melt is plotted as a dashed line in Figure 5. The 1st peak of the XAFS-M3 result is very close to the result of the YCl_3 mixture melt. Figure 6 shows the XAFS function $k^3\chi(k)$ of XAFS-M3, together with the function of molten 5% YCl_3 in the LiCl-KCl eutectic at 773 K. The function of XAFS-M3 is in good agreement with that of the 5% YCl_3 melt in the LiCl-KCl eutectic. These results suggest that Y_2O_3 in the original mixture is converted to YCl_3 and mixed with the LiCl-KCl eutectic melt.

The Zr K-edge Fourier transform magnitudes $|FT(k^3\chi(k))|$ of the XAFS-B, XAFS-M3 and XAFS-A measurements are shown in Figure 7. The magnitude function of the XAFS-B data shows the sharp 1st peak. It is assigned to the 1st Zr^{4+} -Cl⁻ correlation in solid $ZrCl_4$. The nearest Zr^{4+} -Cl⁻ distance obtained from the curve fitting analysis was 2.44 Å. In solid $ZrCl_4$, there are three distinct

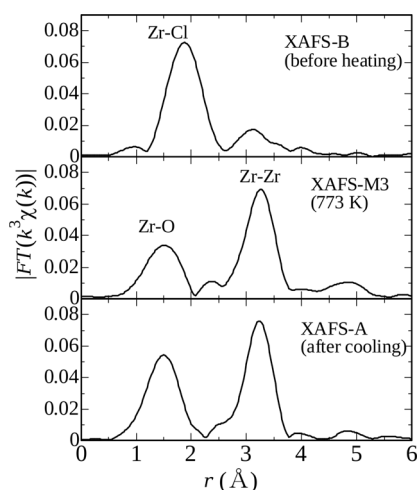


Fig. 7. Fourier transform magnitude function $|FT(k^3\chi(k))|$ of the Zr K-edge for the XAFS-B, the XAFS-M3 and the XAFS-A results.

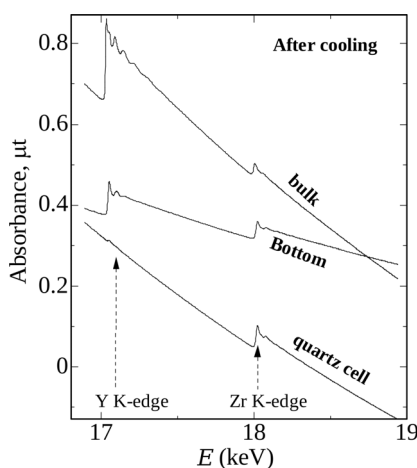


Fig. 8. XAFS spectra of the Y K-edge and Zr K-edge after cooling. In addition to the bulk spectrum, XAFS spectra of a piece of the sample at the bottom of the quartz cell and of the washed quartz cell are shown.

nearest correlation distances; 2.307 Å, 2.498 Å and 2.655 Å [8, 9]. The value of 2.44 Å is relatively close to the averaged one (2.487 Å) of these correlation

distances. Contrasting the chlorination of Y_2O_3 , the starting material $ZrCl_4$ was oxidized at 823 K. The magnitude function of XAFS-M3 shows the broad 1st peak at shorter distance than the XAFS-B result. The strong 2nd peak was found in the XAFS-M3 result. These peaks are assigned to the 1st Zr-O and the 1st Zr-Zr correlations, respectively. Also for the XAFS-A result, the similar profile was found in the magnitude function. Since ZrO_2 is not soluble in the molten LiCl-KCl eutectic and Zr atoms are heavier than LiCl and KCl, it is naturally expected that ZrO_2 is precipitated. However, we detected a small Zr K-edge jump of the XAFS-M3 result and also in the XAFS-A result as shown in the Figure 3.

Figure 8 shows raw XAFS spectra of the XAFS-A sample. In addition to the result based on the bulk (equivalent to the spectrum in the Fig. 3), XAFS spectra of a piece of the sample at the bottom of the cell and of the washed quartz cell window are plotted. From the spectrum of the bottom sample, it can be estimated that a small amount of Y_2O_3 did not take part in the reaction. The XAFS spectrum of the quartz cell suggests that $ZrCl_4$ reacts with the quartz surface.

4. Conclusion

The chlorination reaction of Y_2O_3 with $ZrCl_4$ in LiCl-KCl eutectic melt was investigated by XAFS analysis. The reaction occurred drastically between 773 K and 823 K. It was confirmed that the product after the reaction is equivalent to molten YCl_3 -LiCl-KCl eutectic. It was also detected that a small amount of ZrO_2 remains in the melt. The XAFS study suggests that some $ZrCl_4$ reacts with SiO_2 of the quartz cell.

Acknowledgement

The authors gratefully acknowledge the interest and encouragement of Dr. J. Mizuki and Dr. K. Aoki. The authors also thank Prof. K. Kobayashi and Dr. N. Usami for their support in the Photon Factory.

- [1] T. Koyama, T. Hijikata, T. Usami, T. Inoue, S. Kitawaki, T. Shinozaki, M. Fukushima, and M. Myochin, *J. Nucl. Sci. Tech.* **44**, 382 (2007).
- [2] Y. Sakamura, T. Inoue, T. Iwai, and H. Moriyama, *J. Nucl. Mater.* **340**, 39 (2005).
- [3] Y. Okamoto, M. Akabori, H. Motohashi, H. Shiwaku, and T. Ogawa, *J. Synch. Rad.* **8**, 1191 (2001).
- [4] H. Shiwaku, Y. Okamoto, T. Yaita, K. Minato, S. Suzuki, and H. Tanida, *Z. Naturforsch.* **60a**, 81 (2005).
- [5] Y. Okamoto, M. Akabori, H. Motohashi, A. Itoh, and T. Ogawa, *Nucl. Instr. Meth. Phys. Res. A* **487**, 605 (2002).
- [6] T. Ressler, *J. Synch. Rad.* **5**, 118 (1998).
- [7] J. C. Wasse and P. S. Salmon, *J. Phys. Cond. Matter* **11**, 9293 (1999).
- [8] B. Krebs, *Angew. Chem.* **81**, 120 (1969).
- [9] Y. Okamoto and H. Motohashi, *Z. Naturforsch.* **57a**, 277 (2002).